

UDC 535.326:539.05:539.1.074.4:621.385.6

DOI <https://doi.org/10.32782/pet-2022-2-7>

**Petro TROKHIMCHUCK**

*Ph.D., Associate Professor Associate Professor at Department of A.V. Svidzynskiy's Theoretical and Computer Physics, Lesya Ukrainka Volyn National University, 13 Volya Ave., Lutsk, Ukraine, 43025*

**ORCID ID:** 0000-0003-2737-0506

**SCOPUS-AUTHOR ID:** 8383601100

**To cite this article:** Trokhimchuck, P. (2022). Do pytannia pro pryrodu ta modeliuvannia optychno-indukovanoho cherenkovskoho vyprominiuvannia [To question about nature and modeling the optical-induced Cherenkov radiation]. *Physics and Education Technology*, 2, 44–53. doi: <https://doi.org/10.32782/pet-2022-2-7>

## TO QUESTION ABOUT NATURE AND MODELLING THE OPTICAL-INDUCED CHERENKOV RADIATION

*The main problems of nature the optical-induced Cherenkov radiation are discussed. We show that this problem are connected with problem of shock excitation of heterogeneous polarization the irradiated matter. With this point of view the Cherenkov radiation is Nonlinear Optical (NLO) phenomenon. But classical NLO effects are phenomena with homogeneous shock-excited polarization. Two aspects of modeling this phenomenon are observed. First, microscopic, is based on synthesis A. Bohr theory of representation the Cherenkov radiation on the basis the scattering charge particles in media. This theory gives hyperboloid of the shape of the particle's braking track in the medium. Generating cones of Cherenkov radiation are formed by external normals to the A. Bohr hyperboloid. Second, macroscopic is based on I. Golub model of formal analogy Snell law and Cherenkov radiation. Cherenkov speed is determined as speed of shock nonlinear polarization of irradiated matter. Synthesis A. Bohr and I. Golub models allow to determine the product of nonlinear laser-induced refraction index and speed of nonlinear polarization. The essential difference between optically induced and classical (obtained by gamma quanta or charged particles) Cherenkov radiation lies in the radiation distribution spectrum. The classical spectrum is more homogeneous, since each particle "has" its own hyperboloid. For the optical case, we have the number of cones, which is related to the mode structure of laser radiation. So for the TEM<sub>00</sub> fashion we have only one cone. That is why the radiation spectrum will be more heterogeneous, as in the classic case: ultraviolet radiation will be in the central part, and infrared radiation will be at the edges. The observation of laser-induced Cherenkov radiation is connected with problem of diffraction stratification and known as surface continuum radiation.*

**Key words:** Cherenkov radiation, A. Bohr model, I. Golub model, optical breakdown, Relaxen Optics, cascade processes, shock processes, modeling.

**Петро ТРОХИМЧУК**

*кандидат фізико-математичних наук, доцент, доцент кафедри теоретичної та комп'ютерної фізики імені А. В. Свідзинського, Волинський національний університет імені Лесі Українки, просп. Волі, 13, м. Луцьк, Україна, 43025*

**ORCID ID:** 0000-0003-2737-0506

**SCOPUS-AUTHOR ID:** 8383601100

**Бібліографічний опис статті:** Трохимчук, П. (2022). До питання про природу та моделювання оптично-індукованого черенковського випромінювання. *Фізика та освітні технології*, 2, 44–53, doi: <https://doi.org/10.32782/pet-2022-2-7>

## ДО ПИТАННЯ ПРО ПРИРОДУ ТА МОДЕЛЮВАННЯ ОПТИЧНО-ІНДУКОВАНОГО ЧЕРЕНКОВСЬКОГО ВИПРОМІНЮВАННЯ

*Обговорюються основні проблеми природи оптично-індукованого черенковського випромінювання. Показано, що ця проблема пов'язана з проблемою ударного збудження неоднорідної поляризації опроміненої речовини. З цієї точки зору випромінювання Черенкова є нелінійним оптичним явищем. Але класичні ефекти нелінійної оптики – це явища з однорідною ударно-збуджуваною поляризацією. Спостерігаються два аспекти моделювання цього явища. Перший, мікроскопічний, заснований на теорії О. Бора представлення черенковського випромінювання на основі розсіювання заряджених частинок у середовищах. Ця теорія дає вигляд форми гальмівного шляху частинки в середовищі у вигляді гіперолоїда. Твірні конуси черенковського випромінювання утворені зовнішніми нормальними до гіперолоїда*

*О. Бора. По-друге, макроскопічний базується на моделі І. Голуба формальної аналогії закону Снелла та Черенковського випромінювання. Черенковська швидкість визначається як швидкість ударної нелінійної поляризації опроміненої речовини. Синтез моделей О. Бора та І. Голуба дозволяє визначити добуток нелінійного лазерно-індукованого показника заломлення на швидкість нелінійної поляризації. Істотна відмінність оптично індукованого від класичного (отриманого гамма-квантами або зарядженими частинками) черенковського випромінювання полягає в спектрі розподілу випромінювання. Класичний спектр більш однорідний, оскільки кожна частка «має» свій гіперболіод. Для оптичного випадку ми маємо кількість конусів, яка пов'язана з модовою структурою лазерного випромінювання. Отже, для моди  $TEM_{00}$  ми маємо лише один конус. Тому спектр випромінювання буде більш неоднорідним, як і в класичному випадку: ультрафіолетове випромінювання буде в центральній частині, а інфрачервоне – по краях. Спостереження лазерно-індукованого черенковського випромінювання пов'язане з проблемою дифракційного розширення і відомо як поверхневе континуальне випромінювання.*

**Ключові слова:** черенковське випромінювання, модель О. Бора, модель І. Голуба, оптичний пробій, релаксаційна оптика, каскадні процеси, ударні процеси, моделювання.

## Introduction

Cherenkov radiation (Vavilov–Cherenkov effect) is electromagnetic radiation emitted when a charged particle (such as an electron) passes through a dielectric medium at a speed greater than the phase velocity (speed of propagation of a wavefront in a medium) of light in that medium (Bohr A., 1950; Frank, 1988; Golub, 1990; Jelly, 1958; Trokhimchuck, 2020; Trokhimchuck, 2022). A classic example of Cherenkov radiation is the characteristic blue glow of an underwater nuclear reactor. Its cause is similar to the cause of a sonic boom, the sharp sound heard when faster-than-sound movement occurs. The phenomenon is named after Soviet physicist Pavel Cherenkov (Frank, 1988; Jelly, 1958).

But Cherenkov radiation may be represented as Nonlinear Optical phenomenon two (Trokhimchuck, 2020; Trokhimchuck, 2022). Therefore, we must researched this effect in more widely sense as radiational relaxation of shock nonlinear excited heterogeneous polarization. This determination is more widely as traditional. It conclude various ways of excited this polarization, including laser irradiation.

The main problems of nature the optical-induced Cherenkov radiation are discussed. We show that this problem are connected with problem of shock excitation if heterogeneous polarization the irradiated matter. With this point of view the Cherenkov radiation is Nonlinear Optical (NLO) phenomenon (Trokhimchuck, 2020; Trokhimchuck, 2022). But classical NLO effects are phenomena with homogeneous shock-excited polarization. Two aspects of modeling this phenomenon are observed. First, microscopic, is based on synthesis A. Bohr theory of representation the Cherenkov radiation on the basis the scattering charge particles in media. This theory gives hyperboloid of the shape of the particle's braking track in the medium. Generating

cones of Cherenkov radiation are formed by external normals to the A. Bohr hyperboloid (Bohr A., 1950). Second, macroscopic is based on I. Golub model of formal analogy Snell law and Cherenkov radiation. Cherenkov speed is determined as speed of shock nonlinear polarization of irradiated matter. Synthesis A. Bohr and I. Golub models allow to determine the product of nonlinear laser-induced refraction index and speed of nonlinear polarization (Trokhimchuck, 2020; Trokhimchuck, 2022). The essential difference between optically induced and classical (obtained by gamma quanta or charged particles) Cherenkov radiation lies in the radiation distribution spectrum. The classical spectrum is more homogeneous, since each particle "has" its own hyperboloid. For the optical case, we have the number of cones, which is related to the mode structure of laser radiation. So for the  $TEM_{00}$  fashion we have only one cone. That is why the radiation spectrum will be more heterogeneous, as in the classic case: ultraviolet radiation will be in the central part, and infrared radiation will be at the edges. The observation of laser-induced Cherenkov radiation is connected with problem of diffraction stratification and known as surface continuum radiation (Trokhimchuck, 2020; Trokhimchuck, 2022).

Problems of the observation the Cherenkov radiation and shock processes in matter as Nonlinear (NLO) and Relaxed (RO) Optical processes are connected with acoustic (thermal) and electromagnetic (plasma and Nonlinear optical) nature (Trokhimchuck, 2020; Trokhimchuck, 2022). These processes may be connected with diffractive stratification of laser beam, including self-focusing, self-trapping, and after this generation of supercontinuum radiation (ordered – Cherenkov radiation, and disorder – plasma radiation) (Trokhimchuck, 2020; Trokhimchuck, 2022).

### Concepts, modeling and discussions

On Fig. 1 experimental data, which are received for sodium containing heat-pipe with 20 cm active length and a Hānsh-type 10 kW peak dye laser, are represented. The sodium density was  $10^{14} - 10^{16} \text{ cm}^{-3}$ . The beam of 0,5 cm<sup>-1</sup> bandwidth laser was focused by a lens into the sodium cell after special filtering. The laser intensity at the focus was 10 MW/cm<sup>2</sup> and is sufficient for the formation of self-trapped filaments. The forward emission was photographed by an Alphax B216 camera with f/number of 1,9, placed after the sodium cell without any imaging optics (Golub, 1986). The laser beam was blocked with small on axis disc to prevent over-expose.

The spectral and angular properties of the conical radiation are well-known (Golub, 1986). The cone angle is 1° – 3° and increases as the laser frequency approaches the atomic transition and with increasing sodium density. The cone spectrum is broad (5 – 10 cm<sup>-1</sup>) and is to the red of the transition. For small laser detuning (5 – 10 cm<sup>-1</sup>) the peak of conic emission is detuning. For large laser detuning (6 – 20 cm<sup>-1</sup>) the peak detuning exhibits saturation behavior; the limiting value is at the dispersionless point – 589,4 nm (Golub, 1986).

Two kinds of experiments were performed to establish the surface character of the conical emission. The light changes polarization of initial beam in a linear case, with a direction determines the difference of right and left polarizations. Self-

trapping of laser light close to the transition is due to saturation effects, and this change in polarization is expected to occur inside the filaments, where saturation degree is maximum. In (Golub, 1986) next conclusion was made: conical radiation is generated at a nonsaturated region such as self-trapped filament surface.

The question about spatial coherence of conical radiation was observed in (Golub, 1986). It was found that the angular and spectral distribution of the conical radiation is independent of lens type. The next conclusion was made the conical radiation from various filaments add up incoherently and display no interference pattern.

The data of laser irradiated different 1 – 10 cm – long cells containing H<sub>2</sub>O or D<sub>2</sub>O are represented in Fig. 2 (Golub, 1990). In these experiments a Quantel YG-471 mode-locked laser was used, which produced 22-psec-duration pulses at 1,06 μm of up to 35 mJ energy or its second harmonic 15-psec-duration pulses of 12 mJ energy. A variety of lenses with focal lengths from 2 to 25 cm, capable of producing intensities in the focal spot of up to 10<sup>12</sup> W/cm<sup>2</sup>. Several (usually 5 to 10) filaments were produced by each pulse/ It was easier to produce supercontinuum by focusing the laser beam with long-focal-length lenses into the long cells, and the threshold for supercontinuum in D<sub>2</sub>O was lower than that in H<sub>2</sub>O. The supercontinuum was spread in a circular rainbow, and for 1,06-μm excitation the generated photon energy increases with the off-

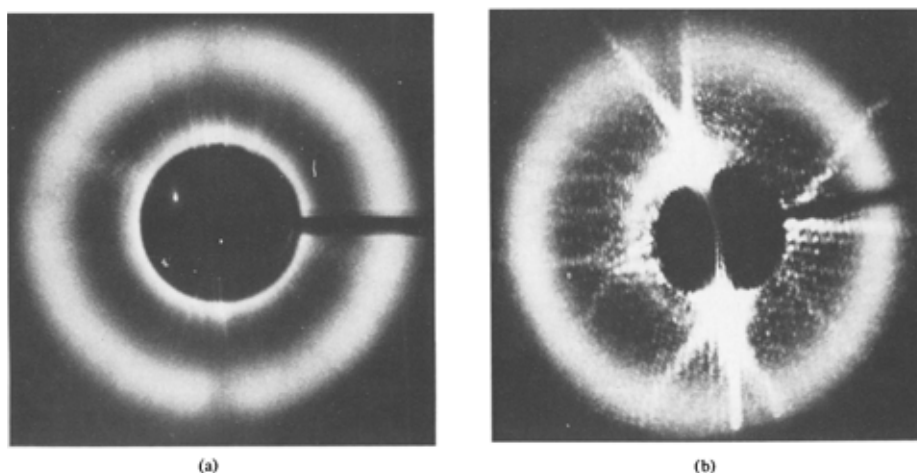


**Fig. 1. The pattern of the conical radiation at sodium density  $1,8 \cdot 10^{15} \text{ cm}^{-3}$  and laser detuning of 0,2 nm to the blue of the D<sub>2</sub> transition. The laser radiation is focused into the sodium cell bay a spherical lens (a) and by a cylindrical lens (b). The laser beam is blocked with a small of on-axis disc. The focal line of the cylindrical lens (b) is the long of horizontal line (Golub, 1986)**

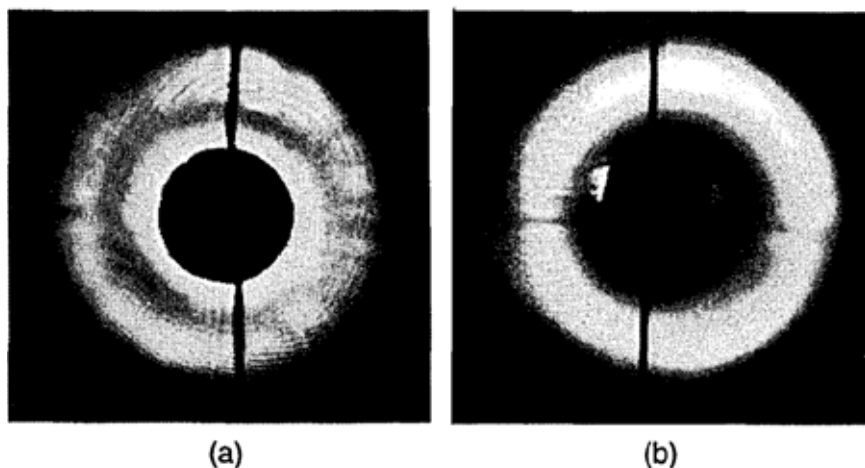


**Fig. 2. Supercontinuum generated in  $D_2O$  by  $0,53\text{-}\mu\text{m}$  laser excitation. The laser is focused into the cell (a) by a spherical lens or (b) by a combination the spherical and cylindrical lenses. The laser beam is blocked with a small of on-axis disc. The focal line of the cylindrical lens (b) is the long of vertical line (Golub, 1990)**

axis angle, while for  $0,53\text{-}\mu\text{m}$  excitation the pattern is more complicated.

Data of Fig. 2 shown that spatial pattern of the supercontinuum conic radiation is independent of the focusing mode, leading one to conclude that the origin of this emission is at the surface of the filaments.

The possibility of generation the Cherenkov radiation in Kerr media was observed in (Trokhimchuck, 2020; Trokhimchuck, 2022). An influence of velocity the motion of self-focusing focus point and self-modulation on frequency-angle spectra of radiation the parametric anti-Stoke component of Brillouin scattering (Trokhimchuck, 2020; Trokhimchuck, 2022). The possibility of generation Cherenkov radiation in this case was proved.

The white-light continuum spectra for various media are represented in (Trokhimchuck, 2020). Ti:sapphire laser system based on the chirped-pulse amplification technique produced a  $1\text{-mJ}$ ,  $70\text{-fs}$  pulse at  $10\text{-Hz}$  repetition rate. The center wavelength was  $785\text{ nm}$ , and the bandwidth was  $20\text{ nm}$ . This fundamental pulse, which had a diameter of  $7\text{ nm}$ , was converted into second- and third-harmonic pulses by doubling and tripling with two  $100\text{-}\mu\text{m}$ -thick  $\beta$ -barium borate crystals. The maximum output energies the second- and third-harmonic pulses were  $180$  and  $30\text{ }\mu\text{J}$ , respectively.

Conic part of filament radiation has continuum spectrum: from ultraviolet to infrared. At first this

effect was called superbroadening. Therefore it may be interpreted as laser-induced Cherenkov radiation (Golub, 1990; Trokhimchuck, 2020; Trokhimchuck, 2022). The angle  $2\theta$  in the vertex of an angle of Fig. 3 (e) is double Cherenkov angle. In this case we have frozen picture of laser-induced destruction of  $4\text{H-SiC}$  (Okada, 2009; Okada, 2012) with help Cherenkov radiation (Trokhimchuck, 2020; Trokhimchuck, 2022).

Imilar results were received for nanosecond  $\text{CO}_2$ -laser irradiation of potassium chloride (Yablonovich, 1971).

The Cherenkov radiation is characterized by two peculiarities (Frank, 1988; Golub, 1990; Jelly, 1958; Trokhimchuck, 2020): 1) creation of heterogeneous shock polarization of matter and, 2) radiation of this polarization. The methods of receiving shock polarization may be various: irradiation by electrons,  $\gamma$ -radiation, ions and excitation with help pulse fields. The stratification of this radiation on other type's radiation (volume, pseudo-Cherenkov a.o.) has relative character and may be represented as laser-induced Cherenkov radiation. Therefore in future we'll be represent conical part of filament radiation as Cherenkov.

This fact may be certified with macroscopic and microscopic ways.

First, macroscopic may be represented according to (Golub, 1990). The similarity between charge particle and light-induced Cherenkov radiation one can invoke the analogy between Snell's law and

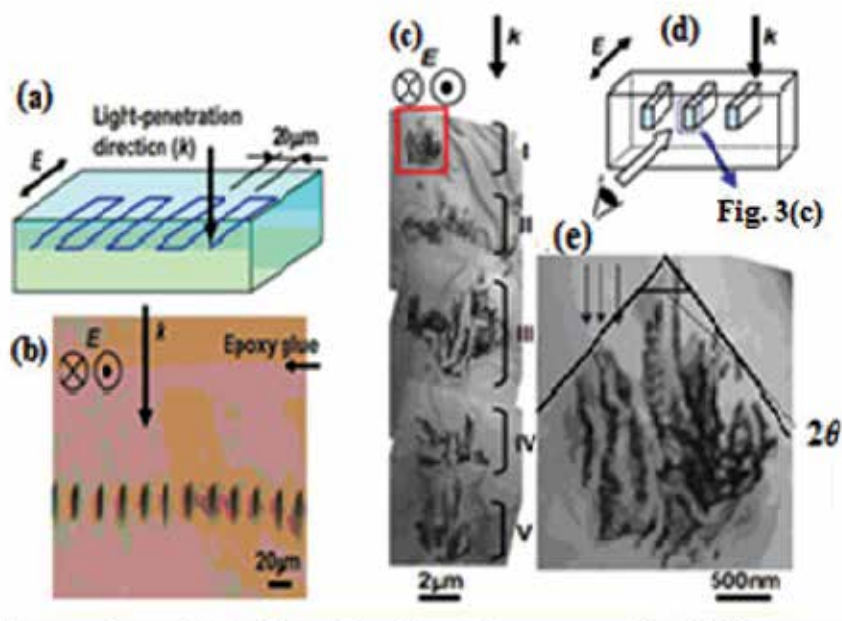


**Fig. 3. (a) Schematic illustration of the laser irradiated pattern. The light propagation  $\theta$  direction ( $k$ ) and electric field ( $E$ ) are shown. (b) Optical micrograph of the mechanically thinned sample to show cross sections of laser-irradiated lines (200 nJ/pulse). (c) Bright-field TEM image of the cross section of a line written with pulse energy of 300 nJ/pulse. (d) Schematic illustration of a geometric relationship between the irradiated line and the cross-sectional micrograph. (e) Magnified image of a rectangular area in (c) (Okada, 2009; Okada, 2012)**

Cherenkov radiation (Golub, 1990). This natural since both effects can be derived in the same way from the Huygens interference principle. In Fig. 4 (a) the point of intersection of a light pulse impinging at an angle  $\varphi$  on a boundary between two media moves with velocity  $V = C/n_1 \cos \varphi$ . This relation with Snell's law, gives the Cherenkov relation (Fig. 4(a)) [1].

$$\cos \theta = C/n_2(\omega)V. \quad (1)$$

This formula allows explain the angle differences for various type of Cherenkov radiation. In this case  $V$  may be represented as velocity of generation the optical-induced polarization too.

Thus the refraction law a light at the boundary between two media is the same as the condition for Cherenkov emission by a source moving along the boundary. In nonlinear medium the emitted frequencies may differ from the excitation frequency. The Cherenkov relation is still valid since the constructive interference occurs at a given Cherenkov angle for each Fourier frequency component of the light-induced nonlinear

polarization. In a sense, one can speak about a nonlinear Snell-Cherenkov effect (Golub, 1990).

The Cherenkov angle  $\cos \theta = C/n_2(\omega)V$  can also be derived from the conservation of the longitudinal component of of the linear momentum at a boundary between two media along which a nonlinear polarization is propagating (Fig. 4 (b)) (Golub, 1990). Using  $k = \omega/V$ , we obtains

$$\cos \theta = k_{nl\ pol}(\omega)/k_{em}(\omega) = V_{em}/V_{nl\ pol} = C/n_2(\omega)V_{nl\ pol}. \quad (2)$$

The role of the boundary can be played by the surface of self-trapped filament. The nonlinear polarization propagating along this surface will result in a light-induced Cherenkov radiation  $\cos \theta = C/n_2(\omega)V$ . The nonconservation of the transverse component of the linear momentum can be related to the uncertainty principle,  $\Delta x \Delta k > 1$ , where  $\Delta x$  is the thickness of the boundary.

The microscopic mechanism of laser-induced Cherenkov radiation is expansion and application of Niels and Aage Bohrs microscopic theory of Cherenkov radiation as part of deceleration radiation on optical case (A. Bohr, 1950; N. Bohr,

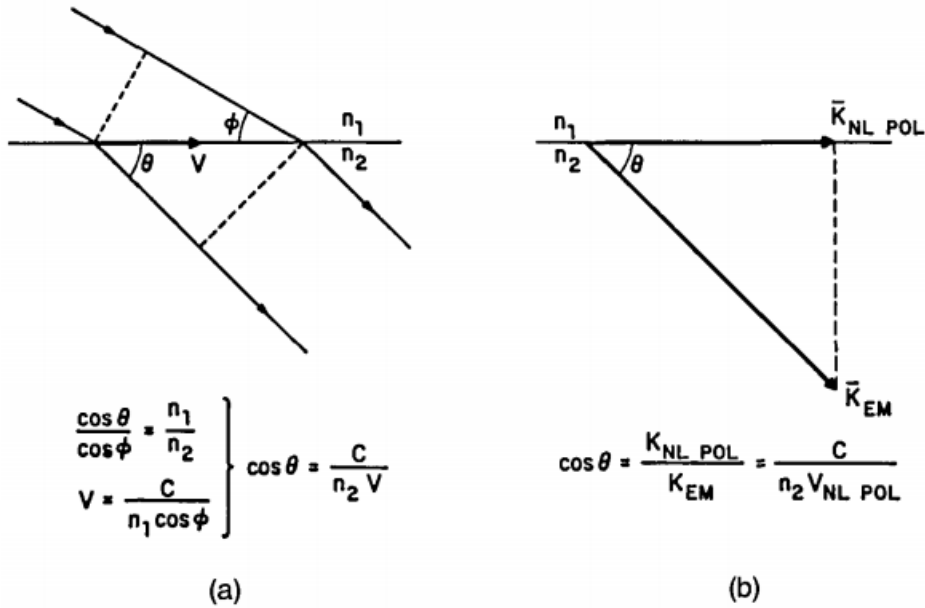


**Fig. 4. (a) Analogy between Snell's law and Cherenkov radiation. The point of intersection of a light pulse impinging upon a boundary two media moves with velocity  $V = \frac{C}{\cos \phi}$ . Combining this relation with Snell's law one obtains the Cherenkov relation,  $\cos \theta = \frac{C}{n_2 V}$ . (b) The Cherenkov angle relation can be obtained from the conservation of the longitudinal component of a linear momentum at a boundary between two media along which a nonlinear polarization is propagated (Golub, 1990).**

1950; Kobzev, 2010). For optical case the Bohrs hyperboloid must be changed on Gaussian distribution of light for mode TEM<sub>00</sub> or distribution for focused light of laser beam (Trokhimchuck, 2020; Trokhimchuck, 2022). In this case Cherenkov angle may be determined from next formula

$$\theta_{Ch} + \alpha_{ir} = \pi/2 \text{ or } \theta_{Ch} = \pi/2 - \alpha_{ir}, \quad (3)$$

where  $\alpha_{ir}$  – angle between tangent line and direction of laser beam.

Focusing (or self-focusing) angle  $\alpha_{ir}$  was determined from next formula

$$\tan \alpha_{ir} = \frac{d_b}{l_{sf}}, \quad (4)$$

where  $d_b$  – diameter of laser beam, (7 mm),  $l_{sf}$  – length of self-focusing. In our case  $\alpha_{ir}$  is angle of focusing or self-focusing (Boyd, 2009; Trokhimchuck, 2020; Trokhimchuck, 2022)

This formula is approximate for average angle  $\alpha_{ir}$ .

The appearance of the conical part of the radiation can be explained on the basis of the microscopic nature of the Cherenkov radiation (A. Bohr, 1950; Frank, 1988; Trokhimchuck, 2020; Trokhimchuck, 2022). The first to draw attention to this were Niels and

Aage Bohr (A. Bohr, 1950; N. Bohr, 1950), and their theory was developed by I. M. Frank and his student A. P. Kobzev (Frank, 1988; Kobzev, 2010). From this point of view, Cherenkov radiation is the inelastic radiation loss of the energy of the incident particle in the medium (A. Bohr, 1950; Frank, 1988; Kobzev, 2010), or in other words, the response of the medium to its polarization by the incident particle.

Fig. 5 shows the scheme that underlies in the N. and A. Bohrs theory (A. Bohr, 1950; N. Bohr, 1950).

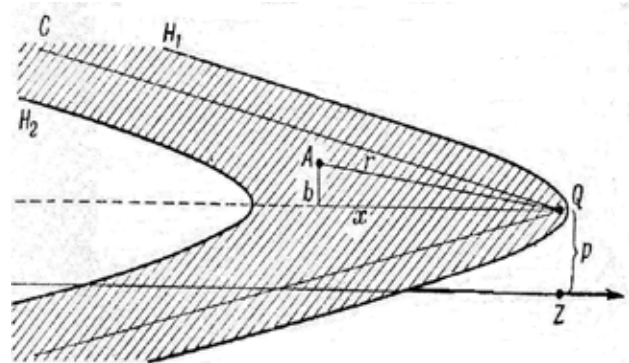


**Fig. 5. To the explanation of the deceleration the particle in a medium (A. Bohr, 1950)**

We will explain on the basis of Fig. 5. Consider an electron that is at a point  $Q$  and collides with a particle  $Z$  that flies at a distance  $p$ . At the same time, the electron is under the influence of the electrons surrounding it, and those electrons that at the moment of time  $t' = t - r/c$  were themselves accelerated give the greatest part of the influence.

The electron at the point  $A$  at time  $t'$  was in such a phase of collision, which is ahead during time  $\tau$  the phase of collision of an electron that is at point  $Q$ . This lead time is equal to (A. Bohr, 1950)

$$\tau = \frac{r}{c} - \frac{x}{\vartheta}. \quad (5)$$

Introduce  $r^2 = x^2 + b^2$  (Fig. 5), we receive from (5) the next correlation

$$\frac{b^2}{\tau^2 c^2 (\gamma^2 - 1)} - \frac{(x + \vartheta \tau \gamma^2)^2}{\vartheta^2 \tau \gamma^2 (\gamma^2 - 1)} = 1, \quad (6)$$

The next conclusion is true: points with a constant  $\tau$  are placed on a hyperboloid. The electrons that "started" or "ended" collisions are placed approximately on hyperboloids  $H_1$  and  $H_2$ , that corresponds to the times  $\tau = -\frac{p}{2\gamma\vartheta}$  and  $\tau = +\frac{p}{2\gamma\vartheta}$ . Thus the main part of the force with which a matter acts on an electron is between the hyperboloids  $H_1$  and  $H_2$ . For the  $\gamma \gg 1$  main part of this region is placed behind the electron at a distance equal or greater than  $p\gamma$ .

The radiation itself occurs in the angle between the perpendiculars to the surface of the hyperboloid, which corresponds to both the angle of the Cherenkov radiation and its broadband. We present a formal theory of this phenomenon according to (A. Bohr, 1950). In this case, the transverse part of the field (between the perpendiculars to the hyperboloid) is characterized by a vector potential, which expands into a Fourier series

$$\vec{A}_r = \sum_{\lambda} q_{\lambda} \vec{A}_{\lambda} + q_{\lambda}^* \vec{A}_{\lambda}^*, \quad \vec{A}_{\lambda} = \sqrt{4\pi c^2 \Omega}^{-1/2} \vec{e}_{\lambda} e^{i(\vec{k}_{\lambda} \cdot \vec{r})}, \quad (7)$$

where values with an asterisk denote complex conjugate values. Here it is assumed that the field is localized in the volume  $\Omega$ ; and the unit vector  $\vec{e}_{\lambda}$  gives the direction of polarization. Amplitudes  $q_{\lambda}$  in formula (7) are not fully determined; they must satisfy even some of the conditions imposed on their dependence on time.

In the approximation of the constant dielectric constant and neglecting the magnetic properties of the matter, we obtain the following equation

$$\Delta \vec{A} - \frac{\varepsilon}{c^2} \frac{\partial^2 \vec{A}}{\partial t^2} = -\frac{4\pi \vec{j}}{c}, \quad (8)$$

where  $\vec{j}$  is the current density, which corresponds to a moving particle;  $\varepsilon$  – dielectric constant of the matter. After multiplying equation (8) by  $\vec{A}_{\lambda}^*$  and integrating over the volume  $\Omega$ , we get

$$(\ddot{q}_{\lambda} + \ddot{q}_{-\lambda}^*) + \omega_{\lambda}^2 (q_{\lambda} + q_{-\lambda}^*) = \frac{z_1 e}{\varepsilon c} (\vec{\vartheta} \cdot \vec{A}_{\lambda}^*(x)), \quad (9)$$

where  $x$  characterizes the position of the particle, which is considered to be a point charge. Frequencies are given by the formula

$$\omega_{\lambda} = \frac{k_{\lambda} c}{\sqrt{\varepsilon}}. \quad (10)$$

Next, we assume that the amplitude  $q_{\lambda}$  dependence on time is harmonic  $\exp(-i\omega_{\lambda} t)$ . As a result of this substitution, equation (9) takes the form

$$\ddot{q}_{\lambda} + \omega_{\lambda}^2 q_{\lambda} = \frac{z_1 e}{2\varepsilon c} \left( 1 + \frac{i}{\omega_{\lambda}} \frac{d}{dt} \right) (\vec{\vartheta} \cdot \vec{A}_{\lambda}^*(x)). \quad (11)$$

If the particle moves at a constant speed, then for  $x = \vartheta t$  the right side of equation (11) it will harmonically depend on time with frequency  $(\vec{k}_{\lambda} \cdot \vec{\vartheta})$ . Equation (11) is reduced to the following equation

$$\ddot{q}_{\lambda} + \omega_{\lambda}^2 q_{\lambda} = \frac{z_1 e}{2\varepsilon c} \left\{ \frac{(\vec{k}_{\lambda} \cdot \vec{\vartheta})}{(\vec{k}_{\lambda} \cdot \vec{\vartheta})} \right\} \left( 1 + \frac{(\vec{k}_{\lambda} \cdot \vec{\vartheta})}{\omega_{\lambda}} \frac{d}{dt} \right) (\vec{\vartheta} \cdot \vec{A}_{\lambda}^*(\vec{\vartheta} t)). \quad (12)$$

Thus, in this particular case, the dispersion of the medium can be taken into account. Only according to equation (12) it is necessary to substitute the value for the dielectric constant, which corresponds to the partial frequency.

As follows from equation (10), in the vacuum the value  $\omega_{\lambda} > (\vec{k}_{\lambda} \cdot \vec{\vartheta})$ , is as  $\vartheta < c$ . In this case, the solution of equation (12) will be forced oscillations with constant amplitude. However, in matter with  $\vartheta > c$  for some wave numbers, we can get  $\omega_{\lambda} = (\vec{k}_{\lambda} \cdot \vec{\vartheta})$ , what corresponds to the resonance between the external force and the oscillator. In this case, the oscillator will continuously absorb energy, which corresponds to the actual Cherenkov radiation. The resonance condition, which is described by formula (10), corresponds to the Cherenkov radiation angle  $\cos\theta = \frac{c}{\vartheta\sqrt{\varepsilon}}$  (A. Bohr, 1950).

Using the Dirac functions, the general solution of equation (12) can be written as follows

$$q_{\lambda} = \frac{z_1 e}{2c\omega_{\lambda}} \frac{1}{\varepsilon \{(\vec{k}_{\lambda} \cdot \vec{\vartheta})\}} \left\{ \frac{1}{\omega_{\lambda} - (\vec{k}_{\lambda} \cdot \vec{\vartheta})} + i\pi\delta(\omega_{\lambda} - \vec{k}_{\lambda} \cdot \vec{\vartheta}) \right\} (\vec{\vartheta} \cdot \vec{A}_{\lambda}^*(\vec{\vartheta} t)). \quad (13)$$

Using equation (13) we determine the force  $\vec{F}_r$  that acts on the particle.

$$\vec{F}_r = -\frac{z_1 e}{c} \dot{\vec{A}}_r(\vec{q}t) = -\frac{z_1 e}{c} \sum_{\lambda} \dot{q}_{\lambda} \vec{A}_{\lambda}(\vec{q}t) + \dot{q}_{\lambda}^* \vec{A}_{\lambda}^*(\vec{q}t), \quad (14)$$

That according (13) give

$$\vec{F}_r = -4\pi^2 z_1^2 e^2 \Omega^{-1} \sum_{\lambda} \vec{e}_{\lambda} (\vec{e}_{\lambda} \cdot \vec{q}) \frac{(\vec{k}_{\lambda} \cdot \vec{q})}{\omega_{\lambda}^2 \{(\vec{k}_{\lambda} \cdot \vec{q})\}} \delta(\omega_{\lambda} - (\vec{k}_{\lambda} \cdot \vec{q})). \quad (15)$$

Summing in two directions of polarization, introducing  $(\vec{k}_{\lambda} \cdot \vec{q}) = k_{\lambda} \vartheta y$  and moving to an infinitely large volume we get (A. Bohr, 1950; Frank, 1988; Kobzev, 2010)

$$F_r = z_1^2 e^2 \int_0^{\infty} k^2 dk \int_{-1}^{+1} \frac{k \vartheta^2 y}{\omega \varepsilon(k \vartheta y)} (1 - y^2) \delta(\omega - k \vartheta y) dy, \quad (16)$$

where  $F_r$  is the force component in the direction of the particle velocity.

In calculating the integral (16), we turn to the new variables,  $\omega$  and  $z = \frac{\vartheta}{c} y \sqrt{\varepsilon(k \vartheta y)}$ . Since  $\vartheta dx dy = d\omega dz$ , we get

$$F_r = \frac{z_1^2 e^2}{c^2} \int_0^{\infty} \omega d\omega \int z \left( 1 - \frac{c^2}{\vartheta^2 \varepsilon(\omega z)} \right) \delta(1 - z) dz, \quad (17)$$

where the last integral is extended to the values of  $z$ , for which  $-1 < \frac{c^2}{\vartheta^2 \varepsilon(\omega z)} < 1$ . This integral is nonzero only for  $z = 1$ , i.e. when the condition is met  $\vartheta \sqrt{\varepsilon(\omega)} > c$ .

Thus, we finally get the value of the force acting on the particle.

$$F_r = \frac{z_1^2 e^2}{c^2} \int_{\vartheta \sqrt{\varepsilon} > c} \left( 1 - \frac{c^2}{\varepsilon \vartheta^2} \right) \omega d\omega, \quad (18)$$

It coincides with the expression obtained by Frank and Tamm for the Cherenkov radiation and its spectral distribution (A. Bohr, 1950; Frank, 1988; Kobzev, 2010).

This model may be used for modeling the optical-induced Cherenkov radiation two. In this case we have more soft regime of excitation this radiation.

Thereby microscopic modified Bohrs theory and macroscopic Golub model are mutually complementary methods.

The decreasing of Cherenkov angle and product  $n_2(\omega) V_{nl\ pol}$  for increasing of laser radiation intensity are corresponded to increasing of nonlinear refractive index and decreasing of velocity of polarization (multiphotonic and multiwave processes).

In whole microscopic mechanism of laser-induced Cherenkov radiation may be represented

as nonequilibrium spectrum of all possible Nonlinear Optical phenomena in the local points of propagation the laser beam. It may be Raman and Brillouin scattering, up- and down-conversion, generation of harmonics and various interference of these processes and phenomena, which are generated the continuous spectrum from ultraviolet to infrared regions (Trokhimchuck, 2020; Trokhimchuck, 2022).

A significant difference between classical and optically induced Cherenkov radiation in the spectral distribution of radiation. This can be explained on the basis of Fig. 5. The spectrum of classical Cherenkov radiation is determined by a set of hyperboloids that characterize the track of each particle. The unevenness of the spectrum is determined by the density of the stream of incoming particles. In the optical case for the single-mode regime, we have one (or several in the case of diffraction stratification) cone (Fig. 3 (c) and Fig. 3 (e)). Therefore, in this case, the spectral distribution of radiation is more heterogeneous, the short-wavelength part of the spectrum is located closer to the center, and the long-wavelength part is located closer to the edges.

From a microscopic point of view, the Mach cone and its angle are determined by the cascade processes of the formation of the nonlinear polarization front, which is caused by a set of nonlinear optical phenomena: from multiphoton absorption to Brillouin to Raman scattering. According to classic electrodynamics (Landau, 1971) maximal value of this angle determined perpendicular to the surface. which are the generators of the Mach cone. The same radiation spreads in the middle of this cone, if "collectivization" ("plasmization" or thermalization) of this process does not occur during the irradiation. Otherwise, the process will be determined by plasma and temperature gradients, and radiation can be generated in different directions (star effect, etc.) (Trokhimchuck, 2020).

Cherenkov radiation with optical pumping may be represented as Nonlinear Optical process with velocity is less as light phase speed in irradiated matter. In this case phase speed in matter has physical nature: it is the electromagnetic speed of "collective" motion the charge particles or charge in matter. Therefore, in local scale we have Nonlinear Optical processes, which are modulated of the Mach cone the Cherenkov radiation (Fig. 3 (c)).

It allows add the Niels and Aage Bohrs theory about microscopic mechanism of Cherenkov radiation (A. Bohr, 1950; Trokhimchuck, 2020; Trokhimchuck, 2022).

### Conclusions

1. Experimental data of continuous conic radiation as optical-induced Cherenkov radiation are analyzed.

2. Comparative analysis of main concepts of Cherenkov radiation are represented.

3. A problem of nature laser-induced Cherenkov radiation is discussed.

4. I. Golub macroscopic model of Cherenkov radiation as analogous of Snell effect is observed.

5. A. Bohr microscopic model was adapted for problem of optical-induced Cherenkov radiation.

6. The synthesis of I. Golub and A. Bohr models was used for the modeling the optical-induced Cherenkov radiation.

7. Some applications of this phenomenon are represented.

### BIBLIOGRAPHY:

1. Бор О. Влияние взаимодействия атомов на прохождение зряженных частиц через вещество. В: Н. Бор. Прохождение атомных частиц через вещество. Москва: Иностранная литература, 1950. с. 105–143.
2. Н. Бор. Прохождение атомных частиц через вещество. Москва: Иностранная литература, 1950. 150 с/
3. Boyd R. W., Lukishova S. G., Shen J.-R., editors. Self-Focusing: Past and Present. Springer Series: Topics in Applied Physics. Vol. 114. New York: Springer, 2009. 605 p.
4. Франк И. М. Излучение Вавилова-Черенкова. Теоретические аспекты. Москва: Наука, 1988. 286 с.
5. Golub I. Optical characteristics of supercontinuum generation. Optics Letters. 1990; 15: 305-307.
6. Golub I., Shuker R., Eres G. On the optical characteristics of the conical emission. Optics Communications. Vol. 57, Is. 2, 1986. – P. 143-145
7. Jelley J. V. Čerenkov radiation and its applications. New York: Pergamon, 1958. 304 p.
8. Кобзев А. П. Механизм Черенковского излучения. Элементарные частицы и атомное ядро, том. 41, вып. 3, 2010. – С. 830-867.
9. Landau L. D., Lifshits E. M. The Classical Theory of Fields. Third Revised English Edition. Course of Theoretical Physics, Volume 2. Oxford, etc.: Pergamon Press, 1971. 387 p.
10. Okada T., Tomita T., Matsuo S., Hashimoto S., Ishida Y., Kiyama S., Takahashi T. Formation of periodic strain layers associated with nanovoids inside a silicon carbide single crystal induced by femtosecond laser irradiation. J. Appl. Phys. 2009 v. 106, p.054307, 2009. – 5 p.
11. Okada T., Tomita T., Matsuo S., Hashimoto S., Kashino R., Ito T. Formation of nanovoids in femtosecond laser irradiated single crystal silicon carbide. Material Science Forum. 2012; 725: 19 – 22.
12. Trokhimchuck P. P. Relaxed Optics: Modelling and Discussions. Saarbrücken: Lambert Academic Press, 2020. 249 p.
13. Trokhimchuck P. P. Relaxed Optics: Modelling and Discussions 2. Saarbrücken, Cisinau: Lambert Academic Press, 2022. 210 p.
14. Yablonovich E. Optical Dielectric Srength of AlkaliHalide Crystals Obtained by Laserinduced Breakdown. Appl. Phys. Lett. 1971; 19: 495-497.

### REFERENCES:

1. Bohr, A. (1950) The influence of atoms interactions on the penetration of particles through matter. In: N. Bohr. The penetration of atomic particles through matter. Moscow: Inostrannaya literatura, pp. 105–143. (In Russian)
2. Bohr, N. (1950) The penetration of atomic particles through matter. Moscow: Inostrannaya literatura, 144 p. (In Russian)
3. Boyd R. W., Lukishova S. G., Shen J.-R., (2009) editors. Self-Focusing: Past and Present. Springer Series: Topics in Applied Physics. Vol. 114. New York: Springer, 605 p.
4. Frank, I. M. (1988) Vavilov-Cherenkov radiation. Theoretical aspects. Moscow: Nauka, 286 p. (In Russian)
5. Golub, I. (1990) Optical characteristics of supercontinuum generation. Optics Letters, vol. 15, pp. 305-307.
6. Golub I., Shuker R., Eres G. (1986) *On the optical characteristics of the conical emission*. Optics Communications, vol. 57, is. 2, pp. 143-145.
7. Jelley, J. V. (1958) Čerenkov radiation and its applications. New York: Pergamon, 304 p.
8. Kobzev, A. P. (2010) Cherenkov radiation mechanism. EPAN, vol.41, is.3, pp. 830-867. (In Russian)
9. Landau L. D., Lifshits E. M. (1971) The Classical Theory of Fields. Third Revised English Edition. Course of Theoretical Physics, Volume 2. Oxford, etc.: Pergamon Press, 387 p.
10. Okada T., Tomita T., Matsuo S., Hashimoto S., Ishida Y., Kiyama S., Takahashi T. (2009) Formation of periodic strain layers associated with nanovoids inside a silicon carbide single crystal induced by femtosecond laser irradiation. J. Appl. Phys., vol. 106, p.054307, 5 p.

11. Okada T., Tomita T., Matsuo S., Hashimoto S., Kashino R., Ito T. (2012) Formation of nanovoids in femtosecond laser irradiated single crystal silicon carbide. *Material Science Forum*, vol. 725, pp. 19 – 22.
12. Trokhimchuck, (2020) P. P. *Relaxed Optics: Modelling and Discussions*. Saarbrücken: Lambert Academic Press, 249 p.
13. Trokhimchuck, P. P. (2022) *Relaxed Optics: Modelling and Discussions 2*. Saarbrücken, Cisinan: Lambert Academic Press, 210 p.
14. Yablonovich E. (1971) Optical Dielectric Strength of AlkaliHalide Crystals Obtained by Laserinduced Breakdown. *Appl. Phys. Lett.*, vol. 19, is. 11, P. 495-497.